

Cite this: *Phys. Chem. Chem. Phys.*, 2012, **14**, 9311–9316

www.rsc.org/pccp

PAPER

The electronic structure of $\text{Ge}_9[\text{Si}(\text{SiMe}_3)_3]_3^-$: a superantiatom complex†‡

P. Andre Clayborne*^a and Hannu Häkkinen*^{ab}

Received 13th October 2011, Accepted 26th January 2012

DOI: 10.1039/c2cp23229d

We report on the electronic structure of $\text{Ge}_9[\text{Si}(\text{SiMe}_3)_3]_3^-$. Systematic density functional theory analysis of the electronic shell structure of the cluster and its derivatives reveals that the $\text{Ge}_9[\text{Si}(\text{SiMe}_3)_3]_3^-$ and its neutral counterpart have electronic shells that can be explained using the superatom model. The ligand–core interaction of these complexes is distinctly different from previously identified gold, gallium, and aluminium superatom complexes, indicating an electron-donating rather than electron-withdrawing ligand. We modify the electron-counting rule for this case and introduce a simple picture for superatom and superantiatom complexes. Discussions comparing shell models, Zintl clusters, the superhalogen Al_{13} and superatom complexes to $\text{Ge}_9[\text{Si}(\text{SiMe}_3)_3]_3^-$ are presented.

Introduction

Zintl anions, known since the work of Joannis in the 1890s, are post-transition metal clusters with the ability to exist in multiple charged states.^{1,2} These clusters isolated in Zintl phases are crystallized with counteranions through various experimental techniques.³ Typically E_9^{x-} Zintl clusters ($\text{E} = \text{Si}, \text{Ge}, \text{Sn}$, and Pb ; $x = 2\text{--}4$) are nine-atom cages whose geometry has been explained primarily using the Wade–Mingos rules to account for the number of vertices on the subsequent cages. Wade–Mingos rules correlate the shape of the cluster with the number of skeletal electrons as first used for boranes and carboranes.⁴ The concept of applying these rules to post-transition metal clusters was realized by Corbett in the 1960's and has since been applied to a series of nine-atom Zintl clusters.⁵

The study of Zintl clusters has grown to include the so-called “functionalization” of germanium clusters.^{6–8} Functionalization requires the addition of an organic substituent to the Ge_9^{4-} cage. For example, the nine-atom germanium cluster ligated by two diphenylbismuth groups was successfully synthesized by Ugrinov and Sevov in 2001.⁶ Sevov and co-workers have illustrated

through the alkenylation of Ge_9 , resulting in a variety of organo-Zintl compounds.⁷ Further, there has been documented success of the Ge_9^{4-} Zintl cluster interacting with transition-metal and noble metal compounds.⁸

Recently, the study of nine-atom germanium clusters and their interaction with ligands has been extended to include metalloid clusters.⁹ Metalloid clusters have metal–metal bonds which outnumber the metal–ligand bonds.¹⁰ Thereby the cluster has both “naked” and ligand-bound atoms. Synthesized by Schnepf, the $\text{Ge}_9\{\text{Si}(\text{SiMe}_3)_3\}_3^-$ cluster (Fig. 1A) and its neutral counterpart have been studied for their uses as molecular cables and building blocks for supramolecular chemistry.^{9,11}

In the case of the Zintl polyanion, Ge_9^{4-} , its stability has primarily been explained within the construct of Wade–Mingos

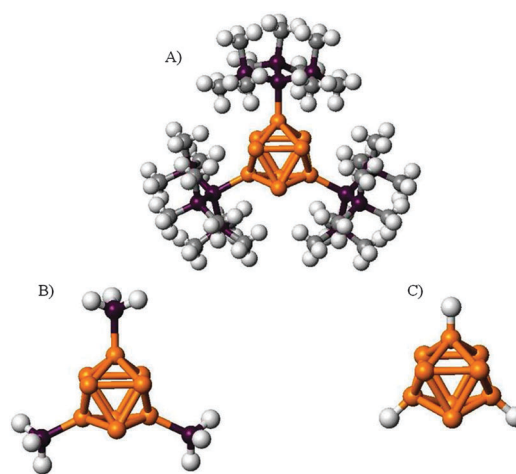


Fig. 1 Relaxed geometries of (A) $\text{Ge}_9[\text{Si}(\text{SiMe}_3)_3]_3^-$ (1), (B) $\text{Ge}_9[\text{SiH}_3]_3^-$ (3) and (C) Ge_9H_3^- (2). The gold, purple, grey and white balls represent the germanium, silicon, carbon and hydrogen atoms, respectively.

^a Department of Chemistry, Nanoscience Center, FI-40014 University of Jyväskylä, P.O. Box 35, Jyväskylä, Finland.

E-mail: penae.a.clayborne@jyu.fi; Fax: +358 14 260 4756

^b Department of Physics, Nanoscience Center, FI-40014 University of Jyväskylä, P.O. Box 35, Jyväskylä, Finland.

E-mail: hannu.j.hakkinen@jyu.fi; Tel: +358 40 024 7973

† This contribution is dedicated to Professor Ludger Wöste for his 65th birthday.

‡ Electronic supplementary information (ESI) available: The structure of 1, 2, and 3 with a table of the bond lengths and dihedral angles and projected density of states for the Ge_9Na_3^- cluster. The table of the HOMO–LUMO gaps for superatoms and superatom complexes. The angular-momentum-projected electron density of states for Ge_9 and $\text{Ge}_9[\text{Si}(\text{SiMe}_3)_3]_3^-$. See DOI: 10.1039/c2cp23229d

rules that correlate geometry and electron count. Occasionally, Zintl clusters have been rationalized using a “jellium”-based model.¹ The jellium model incorporates a positively charged (spherical or non-spherical) background potential to solve the Schrödinger equation, which results in discrete energy levels of the delocalized (“metallic”) electrons that correspond to angular momentum shells (in the spherical case the shells are labeled as: $1S^2 1P^6 1D^{10} 2S^2 1F^{14}, 2P^6, 1G^{18} \dots$).¹² In cases where the electronic shells are filled, the number of electrons (n_e) corresponds to one of the “magic” numbers ($n_e = 2, 8, 18, 20, 40, 58, \dots$), and an energy gap appears in the shell structure, hence these clusters are expected to have an enhanced stability and are analogous to noble atoms on the periodic chart.¹³

The idea of using this “superatom model” has become prudent in explaining the stable nature of not only bare cluster systems, but has extended to include cluster systems stabilized by ligands.^{14–20} These *superatom complexes*, defined as clusters with a metallic core surrounded by organic or organometallic ligands, take the effect of the ligand into account by adding an electron withdrawing term for the electron-counting.^{14,15} The electron-counting rule, referred to as the *superatom complex model*, has proven successful for various cluster systems.^{14–20} For example, in 2007 it was proposed that the crystallographically characterized $Au_{102}(SR)_{44}$ cluster could be understood as a 58-electron superatom; this was followed by computational investigations that identified this cluster as a superatom complex.^{15,16} The $Au_{25}(SR)_{18}^-$ is a superatom complex with 8 delocalized electrons.¹⁷ Experimental and computational groups have shown that the metalloid $Ga_{23}[N(Si(CH_3)_3)_2]_{11}$ is a 58 electron superatom complex.¹⁹ Recently our group has shown that a series of aluminium metalloids, such as $Al_4(C_5H_5)_4$ and $Al_{50}(C_5(CH_3)_5)_{12}$, are superatom complexes.^{14,20} It is interesting to note in each of the aforementioned cases, the superatom complex has contained ligands that withdraw electrons. To our knowledge, there has been no report of a superatom complex with ligands that donate electrons to a cluster core. Such a complex would be distinctly different from previous superatom complexes due to the nature of the ligand–core interaction and may be thought of a *superantiatom complex*; this view is similar to that of the superatom family proposed by Watanabe and Inoshita.²¹ They proposed that a superatom family could exist with semiconductors composed of superatoms, superantiatoms, etc. However, their view incorporated the doping of a semiconductor which would inherently alter the core charge and has previously extended to the doping of various fullerenes.^{21,22} This concept could be applied to superatom complexes albeit not with metallic core doping, but as it pertains to the ligand–core interactions being withdrawing or donating for the superatom and superantiatom, respectively.

The use of the superatom model to describe the stability of the Zintl Ge_9^{4-} and post-transition metalloid clusters has prompted our group to investigate the possibility of a superatomic shell structure for the metalloid $Ge_9\{Si[SiMe_3]_3\}_3^-$ (**1**) (Fig. 1A). To our knowledge there have been no prior detailed theoretical studies into the electronic structure of this cluster complex. We will also compare the electronic shell of **1** with $Ge_9L_3^-$ derivatives as well as give an overview of other electron counting models including Wade–Mingos rules. Finally, a brief discussion of the superatom analogy and

electron counting rules for $Ge_9\{Si[SiMe_3]_3\}_3^-$ and $Ge_9\{Si[SiMe_3]_3\}_3^0$ will be given.

Computational details

The density functional theory calculations were carried out using the Grid-based Projector-Augmented Wave code (GPAW) with the generalized-gradient approximation of Perdew, Burke and Ernzerhof (PBE) to account for the exchange–correlation interaction.^{23,24} $H(1s)$, $C(2s2p)$, $Na(2p3s)$, $Si(3s3p)$ and $Ge(4s4p)$ electrons are treated in the valence with the remaining core electrons being treated using PAW potentials. The electron density is solved in a grid with 0.18 Å spacing. The PAW potential used for the atoms has been compared to literature values for the dimer and atom at various grid spacing, which are within 3% error of experimental values.²³ The $Ge_9\{Si[SiMe_3]_3\}_3^-$ structure (**1**) was obtained from the experimental structure previously reported by Schnepf and fully optimized without symmetry constraints until the residual forces were below $0.05 \text{ eV } \text{\AA}^{-1}$.⁹ The other Ge_9L_m structures reported are based upon the previously reported structure and follow the similar procedure. Each of the relaxed structures is reported in Fig. 1. The Kohn–Sham molecular orbitals were projected on center-of-mass spherical harmonics in a spherical volume of radius R_0 ($R_0 = 3.4 \text{ \AA}$) including the Ge_9 core to analyze the electronic structure.¹⁷ The weights of different angular momenta L (for $L \leq 6$) were calculated as:

$$c_{i,L}(R_0) = \sum_M \int_0^{R_0} r^2 dr |\varphi_{i,LM}(r)|^2$$

and

$$\varphi_{i,LM}(r) = \int d\hat{r} Y_{LM}^*(\hat{r}) \psi_i(r)$$

where i is the index of the Kohn–Sham state and Y_{LM} is the spherical harmonic function. The atomic charges are determined using the Bader analysis.²⁵

Results and discussion

Electronic properties

The fully relaxed geometry of **1** reveals a nine-atom germanium core with a distorted tricapped trigonal prism configuration as previously reported. By comparison, our calculations show good agreement with the experimental structure (Table 1). However, we find that the relaxed structure has slightly longer bond lengths (on average) than what is obtained experimentally, but differs by less than 3%. Previously, the model compound $Ge_9H_3^-$ (**2**) was used as a comparison to gain insight of the electronic properties within the cluster,⁹ however the cluster with

Table 1 Comparison of the experimental and calculated average bond lengths in Ångströms for cluster **1**. The experimental bond lengths come from ref. 9

| | This work | Experimental |
|-------|-----------|--------------|
| Ge–Ge | 2.63 | 2.58 |
| Ge–Si | 2.43 | 2.36 |
| Si–Si | 2.38 | 2.34 |

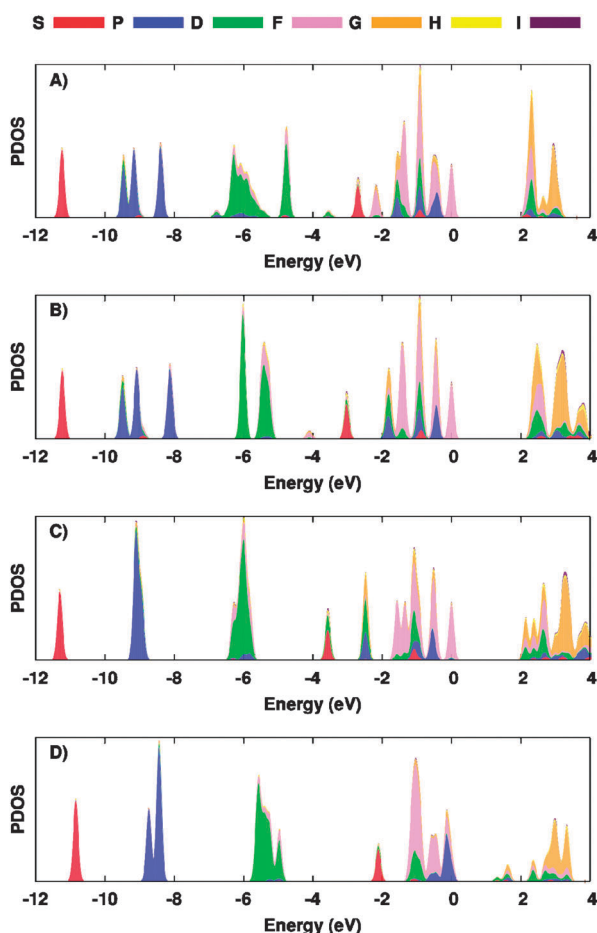


Fig. 2 The angular-momentum-projected electron density of states (PDOS) for $\text{Ge}_9[\text{Si}(\text{SiMe}_3)_3]_3^-$ (**1**) (Panel A), $\text{Ge}_9[\text{SiH}_3]_3^-$ (**3**) (Panel B), Ge_9H_3^- (**2**) (Panel C) and Ge_9Na_3^- (Panel D). Zero corresponds to the highest occupied molecular orbital. The individual electron states are displayed by a Gaussian smoothing of 0.03 eV in the PDOS.

additional model ligands such as $\text{Ge}_9(\text{SiH}_3)_3^-$ (**3**) was omitted. Therefore, we compared **1**, **2**, and **3** to understand the possible effects of the ligand on the electronic properties of the cluster core.

The electronic structure for **1**, **2**, and **3** can be seen in Fig. 2. The electronic structure for **1** (Fig. 2A) illustrates a shell filling with the highest occupied levels having 1F and 2P symmetries. The lower 1P and 1D states show a slight shell splitting. Likewise, **3** (Fig. 2B) does show the similar splitting within the 1P and 1D shells. However, when only hydrogens are used as the ligand (Fig. 2C) the shell splitting of the lower 1P and 1D shells is non-existent, however there is splitting within the 2P shell. The appearance and disappearance of shell splitting within the three cluster compounds brings to light several interesting points. First, the geometry of the cluster core for both **1** and **3** is distorted tricapped trigonal prism configurations. The distortion in **1** and **3** arises from a considerable unsymmetric cluster core as determined by a comparison of the bond lengths and angles between clusters (Table S1, ESI†). However, when only hydrogens are used as a substitute for the full ligand, the nine-atom germanium core transforms into a tricapped trigonal prism with no discernable distortions and

dihedral angles are greater than both **1** and **3**. It is interesting to compare the three systems with the Zintl system Ge_9Na_3^- (Fig. 1D). The Ge_9Na_3^- has a capped quadratic antiprism geometry, different from the previous ligated cluster systems. Analysis of the electronic structure reveals minimal orbital splitting within the 1P, 1D, and 1F, with the 2P states all residing at the HOMO levels for the Ge_9Na_3^- cluster. Thus, the change in the electronic shell can be viewed as a direct effect of the change in the core geometry; this phenomenon has been shown previously in small metallic cluster systems.¹² Second, the ligand choice is important for the properties of the cluster. It was previously proposed that hydrogen atoms are a good representation *in lieu* of a full ligand model, however evidence points that this is not fully correct. If the $\text{Si}(\text{SiMe}_3)$ ligand is replaced by a (SiH_3) ligand, there are minimal changes within the electronic structure and core symmetry. When the full ligand is replaced by only hydrogens, the effect is much greater. Thus, it may be advantageous to substitute organic substituents, but not the full metallo-organic ligands, by only hydrogens to get a good representation of the electronic structure and subsequent properties.

To further investigate the impact of the ligand on the electronic shell of the cluster core (*i.e.* Ge_9), we give the molecular orbitals of Ge_9 , $\text{Ge}_9[\text{Si}(\text{SiMe}_3)_3]_1^-$ and $\text{Ge}_9[\text{Si}(\text{SiMe}_3)_3]_3^-$ clusters (Fig. 3). The Ge_9 cluster using a jellium approach (*i.e.* $n_e = Nv_A$) would have 36 electrons ($n_e = Nv_A$; where $v_A = 4$) which is 2 more than a completely filled 1F shell. When viewing the molecular orbitals, we do find that the 1F shell is completely filled with only one 2P state (HOMO – 3). The LUMO, LUMO + 1 and LUMO + 2

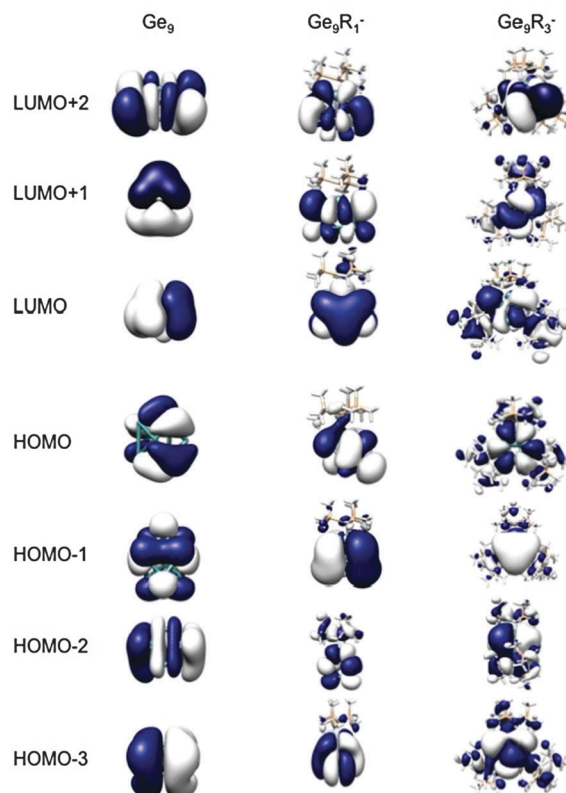


Fig. 3 Kohn–Sham molecular orbitals from HOMO – 3 to LUMO + 2 for Ge_9 , Ge_9R_1^- and Ge_9R_3^- ($\text{R} = \text{Si}(\text{SiMe}_3)_3$).

are the remaining 2P states and the first 1G state is expected within the “superatom” model framework (Fig. 3). The addition of one ligand should yield 37 total electrons (an open shell species), thus for simplicity we add an additional electron for a closed shell species with 38 electrons. According to the projected density of states (Fig. S2, ESI†) and from the molecular orbitals we find that an additional 2P state becomes filled, with only one empty 2P state at the LUMO for $\text{Ge}_9[\text{Si}(\text{SiMe}_3)_3]_1^-$. Also the LUMO + 1 and LUMO + 2 are 1G states. Likewise, once the fully ligated species is obtained the empty 2P state is completely filled (HOMO – 1) as predicted from the projected density of states. It can be seen from the molecular orbitals that there are substantial states where density resides on the ligand as well on the bond between the ligand and cluster core. The fact that there is density on the ligand–core bond illustrates the possible covalent interaction between the ligand and core. It would be interesting to compare the experimentally known Ge_9^{q-} ($q = 2, 3$, and 4) with the increase of ligands to the Ge_9 core (as well as a variety of known ligands), however this is not the focus of the current study.

The density of states with the 40-electron shell closing for **1** illustrates that there is a donation of the electrons to the cluster core. This is further qualitatively supported through Bader charge analysis. The Bader analysis shows that the ligand–core interaction is covalent and with the ligand having an average positive value (+0.7 |e|), with an almost non-polar Ge–Si bond with the silicon having a slightly positive value of (+0.1 |e|). The Bader charge for this system is a similar value to what is found for thiolate-protected gold systems.¹⁹ However, in the thiolate-protected gold clusters the sulfur atom within the ligand has a slightly negative value (–0.1 |e|). The ligand–core interaction is defined as covalent, but the ligand has been deemed as electron withdrawing (which corresponds to the superatom complex model). Therefore, the reported value here is similar, pointing to a covalent bonding situation with the ligand behaving as electron donating to the cluster core. At first this is a surprising result since the previous superatom (metalloid) complexes have each contained electron-withdrawing outer ligand shells. However, the acceptance of charge to the cluster core is typical when comparing **1** to Zintl clusters. Zintl clusters are known for their ability to exist in multiple anionic charged states due to the fluxional ability of the cage. The Ge_9^{q-} cluster is a well studied Zintl system and can accept multiple electrons to its cage.¹

The tensor surface harmonic model and Wade–Mingos rules

Wade–Mingos rules suggest that spherical deltahedral structures with n vertices are stable with $2n + x$ ($x = 2, 4, 6, \dots$) skeletal electrons. The use of this model for many caged deltahedral structures results from the correlation of geometry with the number of skeletal (bonding) electrons which result in the stable behavior of many deltahedral group 14 and 15 clusters. Thus, these rules are electron exclusive by not including non-bonding electrons. In contrast, the jellium model is electron inclusive by taking into account the delocalization of all the valence electrons. For example, using Wade–Mingos rules, the bare Ge_9^{4-} cluster with the capped square antiprism geometry is counted as a 22 skeletal electron nido system. In the jellium model, this cluster

would have a closed shell and 40 valence electrons. This comparison was reported previously by King and Silaghi-Dumitrescu which illustrated how the Ge_9^{4-} cluster contained superatomic states.²⁶ However, in their report it was implied that the jellium model is only relevant when there are no external groups on the cluster of post-transition elements. Thus, we feel it is important to compare these models.

As previously stated, the core can be considered to have donation of three electrons from the ligands with the addition of another electron for the anion. This implies that the core should have 22 electrons similar to the Wade–Mingos view. If one views the electronic structure (Fig. 2A), there is a relatively large energetic separation (2.0 eV) between the core states (HOMO – 35 and HOMO – 16) which appears to support the existence of skeletal electrons; the reason for such a high separation is due to the ligand state residing in-between. However, there are two reasons that dispel the use of Wade–Mingos rules for the germanium core of **1**. First, the structure is a distorted tricapped trigonal prism, reminiscent of a closo-structure instead of the expected nido- (C_{4v} -symmetric monocapped square antiprism) geometry found for the Ge_9^{4-} cluster.¹ Furthermore, when we performed calculations on a typical Zintl cluster compound Ge_9Na_3^- it has the expected nido-geometry and the expected 40-electrons from the jellium model as mentioned previously. The geometry of **1** is neither closo or nido, similar to other reported functionalized Ge_9 clusters, which can be attributed to the ligands on the cluster core.⁶ Secondly, the energy difference between the HOMO – 35 and HOMO – 16 is less than the calculated HOMO–LUMO gap in **1**; thereby supporting the use of an electron inclusive model. Finally, this evidence contradicts the previous assertion of the relevance of the jellium model to only naked post-transition metal clusters, clearly it can be useful to explain the relative stability of a cluster composed of post-transition metal elements interacting with ligands.²⁶

Likewise another shell model, the tensor surface harmonic (TSH) has previously been used to explain many Zintl clusters including endohedral nine-atom clusters.^{1,27} While the TSH model can result in different number of electrons for stability, it can also correspond to similar values found within the superatom (jellium-based) model. The primary difference between the superatom and TSH model is the precise notation of the molecular orbitals. We assert that due to the similarities between the nine-atom cages of E_9^{4-} clusters, the TSH model may be used for the cluster core of **1** and point out that the 40-electron superatom count and model remain intact, similar to the $\text{Cu}@\text{Sn}_9^{3-}$ cluster.²⁸

Comparison with the superhalogen Al_{13}

Reports of the superhalogen Al_{13} in 2005 were based on the resistance of oxygen etching of the anion from gas phase experiments and theoretical calculations.²⁹ Theoretically, the Al_{13}^- cluster was shown to be a forty electron system, with the Al_{13} being one electron short of the closed shell. Also the electron affinity of the Al_{13} cluster was calculated to be 3.4 eV, while the experiment confirmed a high adiabatic electron affinity in the gas phase which illustrated the superhalogen character of the Al_{13} cluster.^{29,30} Likewise, **1** has 40 electrons

and was shown to be unreactive to molecular oxygen in the gas phase.³¹ Therefore its neutral counterpart has 39-electrons and should be similar to the Al_{13} cluster. In order to compare the possibility of $\text{Ge}_9[\text{Si}(\text{SiMe}_3)_3]_3$ as a superhalogen, we calculated the adiabatic and vertical electron affinities. The adiabatic electron affinity is 2.9 eV with the vertical electron affinity slightly higher at 3.1 eV. Though not as high as the Al_{13} cluster system, the electron affinities for $\text{Ge}_9[\text{Si}(\text{SiMe}_3)_3]_3$ are similar to iodine (3.0 eV) and point to its superhalogen character. As with the Al_{13} cluster, superhalogen supramolecules are important in confirming such a possibility.^{29,30} Therefore we point out that several supramolecules have previously been derived, such as $\text{Zn}\{\text{Ge}_9[\text{Si}(\text{SiMe}_3)_3]_3\}_2$ and may be analogous to the zinc iodide compounds in nature, albeit with distinctly different chemical properties.¹¹

Comparison with gold, aluminium and gallium superatom complexes

It is advantageous to compare cluster **1** to other superatom complexes that we have recently analyzed, namely $\text{Au}_{102}(\text{SC}_7\text{O}_2\text{H}_5)_{44}$, $\text{Al}_{50}[\text{C}_5(\text{CH}_3)]_{12}$ and $\text{Ga}_{23}[\text{N}(\text{SiMe}_3)_2]_{11}$.^{14,17,19,20} These superatom complexes have shell closings at 58, 138 and 58, respectively. The HOMO–LUMO gaps (a signature of chemical stability) in these complexes range from 0.5 to 1.3 eV.¹⁹ The calculated HOMO–LUMO gap of **1** is 2.17 eV, greater than any of the aforementioned superatom complexes (Table S1, ESI†). If we compare the isoelectronic superatom complex $\text{Si}@\text{Al}_{14}\text{Cp}_6$ to cluster **1**, we find that the gap is slightly larger by 0.3 eV.¹⁴ It is interesting to note that as the cluster core composition moves across the periodic table (from left to right) for isoelectronic systems, the gap size increases.

The gold, aluminium and gallium superatom complexes have distinctly different ligands, but both the gold and gallium complexes have covalent bonding character, while the aluminium complex has ionic bonding.¹⁹ In order to gain insight into the bonding character of the $\text{Si}(\text{SiMe}_3)_3$ ligand to the germanium core, we performed a Bader analysis. Each of the three Ge atoms has a small negative mean charge ($-0.1 |e|$) indicative of covalent bonding. The absolute value of the charge is similar to the value previously reported for the $\text{Au}_{102}(\text{SC}_7\text{O}_2\text{H}_5)_{44}$ cluster.¹⁹ Until this study, the ligand has been characterized as electron withdrawing from a metallic core in superatom complexes. Thus, the first electron counting rule presented and recently modified by our group would not be satisfactory to explain the number of electrons.^{14,15} Therefore, we introduce a second rule for counting electrons *via*,

$$n_e = N_A v_A + X_L d_L - z \quad (1)$$

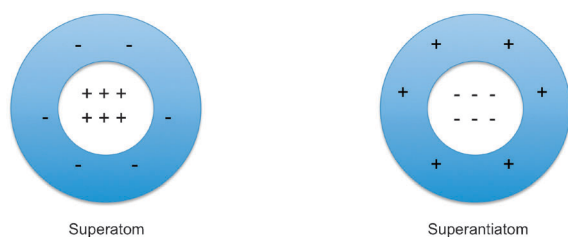


Fig. 4 The simple model picture for superatom and superantiatom complexes.

where the chemical formula would be $[A_N L_X]^z$ while n_e is the number of electrons; N_A is the number of atoms in the core, v_A is the atomic valence (4 for Ge), X_L is the number of ligands, d_L is the number of electrons donated by the ligand and z is the charge of the cluster.

A simple picture model can be derived to illustrate the distinct differences among the family of superatom complexes. In superatom complexes the charge distribution is such that the inner core atoms have a slightly positive charge, with the outer ligand-shell being slightly negative (Fig. 4). Cluster **1** presents a similar charge distribution, however it is reversed. The ligand-shell is positively charged and the core becomes negatively charged (Fig. 4). Thus, to distinguish **1** and possible future cluster complexes of this nature, we introduce the term *superantiatom complex* for these systems.

Conclusions

We have presented a systematic electronic structure analysis of the ligand-stabilized, experimentally known cluster $\text{Ge}_9[\text{Si}(\text{SiMe}_3)_3]_3^-$ and its analogous forms with simpler model ligands. We find that the $\text{Si}(\text{SiMe}_3)_3$ ligand has an electron-donating propensity and that the electronic stability (large HOMO–LUMO gap) of the cluster corresponds to closing of the electron shells at a magic electron number of 40. Simpler model ligands, while yielding a similar overall electronic structure, are not always adequate to stabilize the cluster in the experimentally known geometry. Comparison to previously analyzed ligand-stabilized gold, aluminium and gallium superatom complexes show that the nature of the ligand (electron-withdrawing vs. electron-donating) plays an important role for the electronic structure of the metal core. $\text{Ge}_9[\text{Si}(\text{SiMe}_3)_3]_3^-$ may be characterized as a “superantiatom” complex with a slightly negatively charged core and a positively charged ligand shell.

Acknowledgements

This work was supported financially by the Academy of Finland. The computer resources were provided by the CSC—the Finnish IT Center for Science. We would like to thank Professor Andreas Schnepf for insightful discussions.

Notes and references

- S. Scharfe, F. Kraus, S. Stegmaier, A. Schier and T. F. Fässler, *Angew. Chem., Int. Ed.*, 2011, **50**, 3630.
- N. Korber, *Angew. Chem., Int. Ed.*, 2009, **48**, 3216; T. F. Fässler, *Coord. Chem. Rev.*, 2001, **215**, 347; S. C. Sevov and J. M. Goicoechea, *Organometallics*, 2006, **25**, 5678; J. D. Corbett, *Chem. Rev.*, 1985, **85**, 383; A. Joannis, *C. R. Hebd. Seances Acad. Sci.*, 1891, **113**, 795.
- J. D. Corbett, D. G. Adolphson, D. J. Merryman, P. A. Edwards and F. J. Armatis, *J. Am. Chem. Soc.*, 1975, **97**, 6267; J. D. Corbett, *Angew. Chem.*, 2000, **112**, 682; S. Mandal, R. Lui, A. C. Reber, M. Qian, H. Saavedra, X. Ke, P. Schiffer, S. Sen, P. S. Weiss, S. N. Khanna and A. Sen, *Chem. Commun.*, 2011, **47**, 3126.
- K. Wade, *Inorg. Nucl. Chem. Lett.*, 1972, **8**, 559; D. M. P. Mingos, *Nature (London)*, *Phys. Sci.*, 1972, **236**, 99; K. Wade, *Adv. Inorg. Chem.*, 1976, **18**, 1.
- J. D. Corbett, *Inorg. Chem.*, 1968, **7**, 198.
- A. Ugrinov and S. C. Sevov, *J. Am. Chem. Soc.*, 2001, **124**, 2442.
- M. W. Hull and S. C. Sevov, *Angew. Chem., Int. Ed.*, 2007, **46**, 6695; M. W. Hull and S. C. Sevov, *Inorg. Chem.*, 2007, **46**, 10953; M. W. Hull, A. Ugrinov, I. Petrov and S. C. Sevov, *Inorg. Chem.*, 2007, **46**, 2704; M. M. Gillett-Kunnath, A. G. Oliver and S. C. Sevov, *J. Am. Chem. Soc.*, 2011, **133**, 6560.

- 8 S. Scharfe and T. F. Fassler, *Eur. J. Inorg. Chem.*, 2010, **8**, 1207; B. Zhou, M. S. Denning, C. Jones and J. M. Goicoechea, *Dalton Trans.*, 2009, 1571; E. N. Esenturk, J. Fettinger and B. W. Eichhorn, *J. Am. Chem. Soc.*, 2002, **124**, 4779.
- 9 A. Schnepf, *Angew. Chem., Int. Ed.*, 2003, **42**, 2624; A. Schnepf, *Coord. Chem. Rev.*, 2006, **250**, 2758.
- 10 H. Schnöckel, *Chem. Rev.*, 2010, **110**, 4125.
- 11 C. Schenk and A. Schnepf, *Angew. Chem., Int. Ed.*, 2007, **46**, 5314; A. Schnepf, *Eur. J. Inorg. Chem.*, 2008, 1007; C. Schenk, F. Henke, G. Santiso-Quinones, I. Krossing and A. Schnepf, *Dalton Trans.*, 2008, 4436.
- 12 W. A. de Heer, *Rev. Mod. Phys.*, 1993, **65**, 611.
- 13 A. W. Castleman, Jr., *J. Phys. Chem. Lett.*, 2011, **2**, 1062.
- 14 P. A. Clayborne, O. Lopez-Acevedo, R. L. Whetten, H. Grönbeck and H. Häkkinen, *J. Chem. Phys.*, 2011, **135**, 094701.
- 15 M. Walter, J. Akola, O. Lopez-Acevedo, P. D. Jadzinsky, G. Calero, C. J. Ackerson, R. L. Whetten, H. Grönbeck and H. Häkkinen, *Proc. Natl. Acad. Sci. U. S. A.*, 2008, **105**, 9157.
- 16 P. D. Jadzinsky, G. Calero, C. J. Ackerson, D. A. Bushnell and R. D. Kornberg, *Science*, 2007, **318**, 5849.
- 17 J. Akola, M. Walter, R. L. Whetten, H. Häkkinen and H. Grönbeck, *J. Am. Chem. Soc.*, 2008, **130**, 3756.
- 18 R. B. Dong, X. Chen, H. X. Zhao, X. F. Wang, H. B. Shu, Z. L. Ding and L. Wei, *Phys. Chem. Chem. Phys.*, 2011, **13**, 3274; M. Walter, M. Moseler, R. L. Whetten and H. Häkkinen, *Chem. Sci.*, 2011, **2**, 1583; C. M. Aikens, *J. Phys. Chem. Lett.*, 2011, **2**, 99.
- 19 D. Schebarchov and N. Gaston, *Phys. Chem. Chem. Phys.*, 2011, **13**, 21109; O. Lopez-Acevedo, P. A. Clayborne and H. Häkkinen, *Phys. Rev. B: Condens. Matter Mater. Phys.*, 2011, **84**, 035434; J. Hartig, A. Stösser, P. Hauser and H. Schnöckel, *Angew. Chem., Int. Ed.*, 2007, **46**, 1658.
- 20 P. A. Clayborne, O. Lopez-Acevedo, R. L. Whetten, H. Grönbeck and H. Häkkinen, *Eur. J. Inorg. Chem.*, 2011, **17**, 2649.
- 21 H. Watanabe and T. Inoshita, *Optoelectron.-Devices Technol.*, 1986, **1**, 33.
- 22 S. Osawa, M. Harada and E. Osawa, *Fullerene Sci. Technol.*, 1995, **3**, 225; H. Shinohara, *Rep. Prog. Phys.*, 2000, **63**, 843.
- 23 J. J. Mortensen, L. Hansen and K. W. Jacobsen, *Phys. Rev. B: Condens. Matter Mater. Phys.*, 2005, **71**, 035109; J. Enkovaara, C. Rostgaard, J. J. Mortensen, J. Chen, M. Dulak, L. Ferrighi, J. Gavnholt, C. Glinsvad, V. Haikola, H. Hansen, H. Kristoffersen, M. Kuisma, A. Larsen, L. Lehtovaara, M. Ljungberg, O. Lopez-Acevedo, P. Moses, J. Ojanen, T. Olsen, V. Petzold, N. Romero, J. Stausholm-Møller, M. Strange, G. Tritsarlis, M. Vanin, M. Walter, B. Hammer, H. Häkkinen, G. Madsen, R. Nieminen, J. Nørskov, M. Puska, T. Rantala, J. Schiøtz, K. Thygesen and K. W. Jacobsen, *J. Phys.: Condens. Matter*, 2010, **22**, 253202; M. Walter, H. Häkkinen, L. Lehtovaara, M. Puska, J. Enkovaara, C. Rostgaard and J. J. Mortensen, *J. Chem. Phys.*, 2008, **128**, 244101; the GPAW code is freely available at <https://wiki.fysik.dtu>.
- 24 J. P. Perdew, K. Burke and M. Ernzerhof, *Phys. Rev. Lett.*, 1996, **77**, 3865.
- 25 R. F. W. Bader, *Atoms in molecules*, Clarendon Press, Oxford, 1990; W. Tang, E. Sanville and G. Henkelman, *J. Phys.: Condens. Matter*, 2009, **21**, 236.
- 26 R. B. King and I. Silaghi-Dumitrescu, *Dalton Trans.*, 2008, 6083.
- 27 A. J. Stone, *Inorg. Chem.*, 1981, **20**, 563; A. J. Stone, *Mol. Phys.*, 1980, **41**, 1339; A. J. Stone, *Polyhedron*, 1984, **3**, 1299; R. L. Johnston and D. M. P. Mingos, *Theor. Chim. Acta*, 1989, **75**, 11.
- 28 S. Scharfe, T. F. Faessler, S. Stegmaier, S. D. Hoffmann and K. Ruhland, *Chem.-Eur. J.*, 2008, **14**, 4479.
- 29 D. E. Bergeron, A. W. Castleman Jr, T. Morisato and S. N. Khanna, *Science*, 2004, **304**, 84; D. E. Bergeron, P. J. Roach, A. W. Castleman, N. O. Jones and S. N. Khanna, *Science*, 2005, **307**, 231.
- 30 A. W. Castleman and S. N. Khanna, *J. Phys. Chem. C*, 2009, **113**, 2664; P. Clayborne, N. O. Jones, A. C. Reber, J. U. Reveles, M. C. Qian and S. N. Khanna, *J. Comput. Methods Sci. Eng.*, 2007, **7**, 417.
- 31 C. Schenk, F. Henke, M. Neumaier, M. Olzmann, H. Schnöckel and A. Schnepf, *Z. Anorg. Allg. Chem.*, 2010, **636**, 1173.